Shedding Light on the Origin of ^{204}Pb, the Heaviest s-Process–Only Isotope in the Solar System

A. Casanovas-Hoste [1,2,3,*] C. Domingo-Pardo,[2] J. Lerendegui-Marco,[4] C. Guerrero,[4] A. Tarifeño-Saldivia,[2] M. Krtička,[5] M. Pignatari,[6,7,8,9] F. Calviño,[1] D. Schumann,[10] S. Heinitz,[10] R. Dressler,[10] U. Köster,[11] O. Aberle,[3] J. Andrzejewski,[12] L. Audouin,[13] V. Bécares,[14] M. Bacak,[15] J. Balibrea-Correa,[14] M. Barbagallo,[16] S. Barros,[17] F. Bečvář,[5] C. Beinrucker,[18] E. Berthoumieux,[19] J. Billowes,[20] D. Bosnar,[21] M. Brugger,[3] M. Caamaño,[22] M. Calviani,[3] D. Cano-Ott,[14] R. Cardella,[3] D. M. Castelluccio,[23,24] F. Cerutti,[3] Y. H. Chen,[13] E. Chiaveri,[3] N. Colonna,[16] G. Cortés,[1] M. A. Cortés-Giraldo,[4] L. Cosentino,[25] L. A. Damone,[16,26] M. Diakaki,[19] E. Dupont,[19] I. Durán,[22] B. Fernández-Domínguez,[22] A. Ferrari,[3] P. Ferreira,[17] P. Finocchiaro,[25] V. Furman,[27] K. Göbel,[18] A. R. García,[14] A. Gawlik-Ramięga,[12] T. Glodariu,[28,†] I. F. Gonçalves,[17] E. González-Romero,[14] A. Goverdovski,[29] E. Griesmayer,[15] F. Gunsing,[19,3] H. Harada,[30] T. Heftrich,[18] J. Heyse,[31] D. G. Jenkins,[32] E. Jericha,[15] F. Käppeler,[33,†] Y. Kadi,[3] T. Katabuchi,[34] P. Kavrigin,[15] V. Ketlerov,[29] V. Khryachkov,[29] A. Kimura,[30] N. Kivel,[10] M. Kokkoris,[35] E. Leal-Cidoncha,[22] C. Lederer-Woods,[36] H. Leeb,[15] S. Lo Meo,[23,24] S. J. Lonsdale,[36] R. Losito,[3] D. Macina,[3] J. Marganiec,[12] T. Martínez,[14] C. Massimi,[24,37] P. Mastinu,[38] M. Mastromarco,[16] F. Matteucci,[39,40] E. A. Maugeri,[10] E. Mendoza,[14] A. Mengoni,[23] P. M. Milazzo,[39] F. Mingrone,[24] M. Mirea,[28,†] S. Montesano,[3] A. Musumarra,[25,41] R. Nolte,[42] A. Oprea,[28] N. Patronis,[43] A. Pavlik,[44] J. Perkowski,[12] I. Porras,[3,45] J. Praena,[4,45] J. M. Quesada,[4] K. Rajeev,[46] T. Rauscher,[47,48] R. Reifarth,[18] A. Riego-Perez,[49] Y. Romanets,[17] P. C. Rout,[46] C. Rubbia,[3] J. A. Ryan,[20] M. Sabaté-Gilarte,[3,4] A. Saxena,[46] P. Schillebeeckx,[31] S. Schmidt,[18] P. Sedyshev,[27] A. G. Smith,[20] A. Stamatopoulos,[35] G. Tagliente,[16] J. L. Tain,[2] L. Tassan-Got,[13] A. Tsinganis,[35] S. Valenta,[5] G. Vannini,[24,37] V. Variale,[16] P. Vaz,[17] A. Ventura,[24] V. Vlachoudis,[3] R. Vlastou,[35] A. Wallner,[50] S. Warren,[20] M. Weigand,[18] C. Weiss,[3,15] C. Wolf,[18] P. J. Woods,[36] T. Wright,[20] and P. Žugec[21,3]

(n_TOF Collaboration)

^{1}*Institut de Tècniques Energètiques (INTE)—Universitat Politècnica de Catalunya, Barcelona, Spain*
^{2}*Instituto de Física Corpuscular, CSIC—Universidad de Valencia, Valencia, Spain*
^{3}*European Organization for Nuclear Research (CERN), Switzerland*
^{4}*Universidad de Sevilla, Sevilla, Spain*
^{5}*Charles University, Prague, Czech Republic*
^{6}*Konkoly Observatory, HUN-REN, Konkoly Thege Miklós út 15-17, H-1121 Budapest, Hungary*
^{7}*MTA Centre of Excellence, Budapest, Konkoly Thege Miklós út 15-17, H-1121, Hungary*
^{8}*E. A. Milne Centre for Astrophysics, University of Hull, Hull, United Kingdom*
^{9}*NuGrid Collaboration‡*
^{10}*Paul Scherrer Institut (PSI), Villigen, Switzerland*
^{11}*Institut Laue-Langevin (ILL), Grenoble, France*
^{12}*University of Lodz, Lodz, Poland*
^{13}*Institut de Physique Nucléaire, CNRS-IN2P3, Université Paris-Sud, Université Paris-Saclay, F-91406 Orsay Cedex, France*
^{14}*Centro de Investigaciones Energéticas Medioambientales y Tecnológicas (CIEMAT), Spain*
^{15}*TU Wien, Atominstitut, Stadionallee 2, 1020 Wien, Austria*
^{16}*Istituto Nazionale di Fisica Nucleare, Sezione di Bari, Bari, Italy*
^{17}*Instituto Superior Técnico, Lisbon, Portugal*
^{18}*Goethe University Frankfurt, Frankfurt, Germany*
^{19}*CEA Irfu, Université Paris-Saclay, F-91191 Gif-sur-Yvette, France*
^{20}*University of Manchester, Manchester, United Kingdom*
^{21}*Department of Physics, Faculty of Science, University of Zagreb, Zagreb, Croatia*
^{22}*University of Santiago de Compostela, Spain*
^{23}*Agenzia Nazionale per le Nuove Tecnologie (ENEA), Bologna, Italy*
^{24}*Istituto Nazionale di Fisica Nucleare, Sezione di Bologna, Bologna, Italy*
^{25}*INFN Laboratori Nazionali del Sud, Catania, Italy*

*Contact author: adria.casanovas@upc.edu
†Deceased
‡http://nugridstars.org

[26]Dipartimento Interateneo di Fisica, Università degli Studi di Bari, Bari, Italy

[27]Affiliated with an institute (or an international laboratory) covered by a cooperation agreement with CERN

[28]Horia Hulubei National Institute of Physics and Nuclear Engineering, Romania

[29]Institute of Physics and Power Engineering (IPPE), Obninsk, Russia

[30]Japan Atomic Energy Agency (JAEA), Tokai-Mura, Japan

[31]European Commission, Joint Research Centre (JRC), Geel, Retieseweg 111, B-2440 Geel, Belgium

[32]University of York, York, United Kingdom

[33]Karlsruhe Institute of Technology, Campus North, IKP, 76021 Karlsruhe, Germany

[34]Tokyo Institute of Technology, Tokyo, Japan

[35]National Technical University of Athens, Athens, Greece

[36]School of Physics and Astronomy, University of Edinburgh, Edinburgh, United Kingdom

[37]Dipartimento di Fisica e Astronomia, Università di Bologna, Bologna, Italy

[38]Istituto Nazionale di Fisica Nucleare, Sezione di Legnaro, Legnaro, Italy

[39]Istituto Nazionale di Fisica Nucleare, Sezione di Trieste, Trieste, Italy

[40]Dipartimento di Astronomia, Università di Trieste, Trieste, Italy

[41]Dipartimento di Fisica e Astronomia, Università di Catania, Catania, Italy

[42]Physikalisch-Technische Bundesanstalt (PTB), Bundesallee 100, 38116 Braunschweig, Germany

[43]University of Ioannina, Ioannina, Greece

[44]University of Vienna, Faculty of Physics, Vienna, Austria

[45]University of Granada, Granada, Spain

[46]Bhabha Atomic Research Centre (BARC), India

[47]Centre for Astrophysics Research, University of Hertfordshire, Hatfield, United Kingdom

[48]Department of Physics, University of Basel, Basel, Switzerland

[49]Universitat Politècnica de Catalunya, Barcelona, Spain

[50]Australian National University, Canberra, Australia

Asymptotic giant branch stars are responsible for the production of most of the heavy isotopes beyond Sr observed in the solar system. Among them, isotopes shielded from the r-process contribution by their stable isobars are defined as s-only nuclei. For a long time the abundance of ^{204}Pb, the heaviest s-only isotope, has been a topic of debate because state-of-the-art stellar models appeared to systematically underestimate its solar abundance. Besides the impact of uncertainties from stellar models and galactic chemical evolution simulations, this discrepancy was further obscured by rather divergent theoretical estimates for the neutron capture cross section of its radioactive precursor in the neutron-capture flow, ^{204}Tl ($t_{1/2} = 3.78$ yr), and by the lack of experimental data on this reaction. We present the first ever neutron capture measurement on ^{204}Tl, conducted at the CERN neutron time-of-flight facility n_TOF, employing a sample of only 9 mg of ^{204}Tl produced at the Institute Laue Langevin high flux reactor. By complementing our new results with semiempirical calculations we obtained, at the s-process temperatures of $kT \approx 8$ keV and $kT \approx 30$ keV, Maxwellian-averaged cross sections (MACS) of 580(168) mb and 260(90) mb, respectively. These figures are about 3% lower and 20% higher than the corresponding values widely used in astrophysical calculations, which were based only on theoretical calculations. By using the new ^{204}Tl MACS, the uncertainty arising from the ^{204}Tl(n, γ) cross section on the s-process abundance of ^{204}Pb has been reduced from $\sim$30% down to $+8\%/-6\%$, and the s-process calculations are in agreement with the latest solar system abundance of ^{204}Pb reported by K. Lodders in 2021.

Since the observation of technetium in the stellar atmosphere of R-Andromedae [1] and the emergence of the subsequent theory of synthesis of elements in stars [2,3], the study of asymptotic giant branch (AGB) stars has played an important role in disentangling the origin of the elements beyond iron. Indeed, due to the activation of the slow neutron-capture process (s process), AGB stars are one of the main sources of nuclei heavier than Sr [4–6]. The solar isotopic composition is the best known abundance distribution, and it is a crucial benchmark to study the galactic chemical evolution (GCE) of the Milky Way [7–9]. In particular, the isotopic pattern of heavy elements is derived mainly from Ivuna-type carbonaceus (CI) chondrites analysis, and its precise measurement is a very active
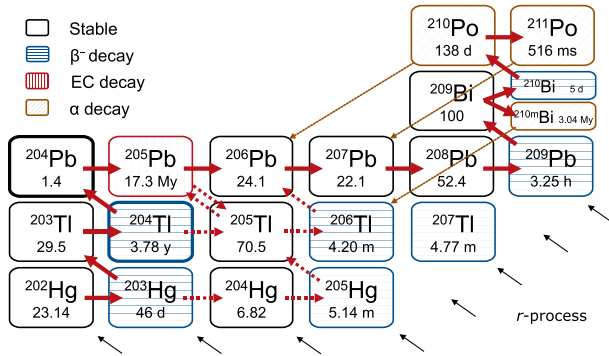
FIG. 1. Schematic view of the chart of nuclei at the termination of the s process. The arrows correspond to the main s-process path, with dashed arrows depicting paths strongly enhanced during high temperature and high neutron density events.

field of research [10]. This pattern is the result of GCE driven by multiple generations of stars and different nucleosynthesis mechanisms. However, it is possible to identify nuclei that are produced almost entirely by the s process, since they are shielded from contributions of the rapid neutron-capture process (r process), which is the other main mechanism contributing to the formation of heavy nuclei [11]. These so-called s-only isotopes play a pivotal role in studying the s-process nucleosynthesis in AGB stars and in validating stellar models at different metallicities [7,12–15]. ^{204}Pb is the heaviest s-only isotope and thus it serves to benchmark state-of-the-art AGB models in the heavy-mass region around neutron magic number $N = 126$, corresponding to the s-process peak in the Pb-Bi region. Also, ^{204}Pb is the single lead isotope that preserves its primordial abundance, thus enabling the Pb-Pb chronometry of the early Solar System [16,17]. As it can be inferred from Fig. 1 the production of ^{204}Pb is directly affected by the interplay between the β^--decay rate and the neutron capture cross section of the unstable ^{204}Tl ($t_{1/2} = 3.78$ yr), which acts as a branching point in the s-process path. Until now, apart from a transmission measurement from 1968 [18] in the 0.2 eV to 1 keV energy range, only theoretical calculations of the Maxwellian-averaged cross section (MACS) of ^{204}Tl(n, γ) were available [19]. The latter differ from each other by more than a factor of 2 at $kT = 30$ keV, i.e., from 97 mb [20] to the value of 224(78) mb estimated by TENDL-2021 [21]. An estimation of 134 ± 40 mb was obtained from the interpolation of time-of-flight (TOF) measurements of the neighboring isotopes ^{203}Tl and ^{205}Tl at ORNL [22]. Finally, the value of 215 ± 38 mb recommended by the KADoNiS v0.3 database [19], commonly used as reference for nucleosynthesis calculations, corresponds to a previous theoretical calculation by Bao et al. obtained with the NON-SMOKER code [23]. Note that the uncertainty of 18% quoted there is rather questionable in view of the large discrepancies among different theoretical estimates [19].

Previous nucleosynthesis calculations based on the KADoNiS v0.3 ^{204}Tl MACS found a systematic underproduction of the solar abundance of ^{204}Pb [12,14,15,24]. Some of the missing ^{204}Pb could have been produced by the γ process in supernovae [25–27]. However, the origin of this process in stars is still matter of debate and its GCE contribution to ^{204}Pb still remains rather uncertain [28]. Another possible explanation of the predicted deficiency could be a yet unidentified fractionation mechanism operating in the early solar system. By comparing the observed solar abundances with nearby solar twins, Gonzalez [29] suggested the corrections to the elemental meteoritic abundances needed to take this effect into account. For the case of Pb, this led to a reduction of the Pb/Sm elemental ratio of $\log_{10}(\text{Pb}/\text{Sm}) = -0.1$.

As described by Bisterzo et al. [15], a reliable assessment of additional nucleosynthesis contributions to ^{204}Pb from other stellar sources and/or fractionation effects has been hindered by the uncertainty in the thermal dependency of the β^--decay rate [30,31], and most importantly, by the large uncertainty in the neutron capture cross section of ^{204}Tl and the lack of experimental data.

However, direct measurements on radioactive isotopes are very challenging. When the reaction product is stable and thus the sensitive activation technique cannot be applied, the TOF technique represents the only alternative. Thus far, from the 21 key s-process branching nuclei discussed by Käppeler et al. [5], it has been successfully applied only to ^{63}Ni [32], ^{79}Se [33], ^{151}Sm [34], and ^{171}Tm [35]. Of these nuclei only the last has a very short half-life (1.92 yr) comparable to that of ^{204}Tl.

In this work, the ^{204}Tl sample was produced from a machine-pressed pellet of Tl$_2$O$_3$ containing 225 mg of thallium, enriched up to 99.5% in ^{203}Tl. This pellet was irradiated for 55 days in the high flux reactor of the Institute Laue Langevin (ILL). From the initial seed composition and the irradiation parameters, the content of ^{204}Tl at the time of the experiment was calculated to be 9.0(5) mg, corresponding to an enrichment of 4.0(2)%. Prior to the irradiation at ILL, the pellet had been enclosed in a sealed quartz capsule in order to avoid any loss of material. The capsule was cylindrical in shape, with a length of 30 mm, an external diameter of 8 mm, and 1 mm thick walls.

The capture experiment was performed at the CERN neutron time-of-flight facility, n_TOF [36]. At n_TOF pulses of neutrons are produced by the spallation reactions induced by a 20 GeV/c proton beam impinging a massive lead target, with the neutron energy E_n determined by applying the TOF technique. The experiment was conducted at the 185 m neutron beam line of the Experimental Area 1 (EAR1). This beam line offers the best combination among all current world TOF facilities in terms of high instantaneous neutron flux and long flight path [37], which allows us to achieve a resolution of $\Delta E_n/E_n = 10^{-3}$ or better in the E_n range between 1 eV and 10 keV [36].

The neutron capture yield was measured by detecting the prompt deexcitation γ rays emitted after each capture event, employing the n_TOF standard setup of four C_6D_6 liquid scintillation detectors [38], which are optimized to minimize their neutron sensitivity [39]. Lead foils were placed on the detectors to reduce the impact of the low energy bremsstrahlung γ rays arising from the ^{204}Tl decay. The γ-ray cascade detection efficiency was rendered proportional to the total energy of the cascade E_C, and thus independent of the particular deexcitation path of the cascade, by applying the pulse height weighting technique (PHWT) [40–42]. The application of the PHWT required detailed MC simulations of the detection setup response to a wide range of γ-ray energies, performed with the GEANT4 toolkit [43–45]. After applying the PHWT, the experimental capture yield can be expressed as

$$Y_{\exp}(E_n) = f_{\text{th}} \cdot f_N \cdot \frac{C_w(E_n) - B_w(E_n)}{\phi(E_n) \cdot E_C}. \quad (1)$$

Here, $C_w(E_n)$ and $B_w(E_n)$ are the weighted total and background counts, respectively, while $\phi(E_n)$ is the neutron fluence, derived from the energy dependence of the n_TOF neutron flux [46].

The background counts, $B_w(E_n)$, had two dominant components, which were assessed separately. The counts generated by the activity of the sample were evaluated by acquiring data with the sample and without neutron beam. The second, beam induced background component, mostly originating from the capture of beam neutrons scattered mainly by the sample quartz container, was evaluated by measuring an identical empty container.

The absolute normalization factor, f_N, accounts for the fraction of beam intersecting the sample. For the ^{204}Tl-enriched sample, the determination of f_N required us to consider the spatial distribution of activated material inside the capsule and thus, f_N was obtained in a two-step process. First, a separate measurement using a highly enriched ^{203}Tl sample was conducted to determine the capture area A_r of ^{203}Tl(n, γ) resonances. A_r is defined as [47]

$$A_r = 2\pi^2 \lambdabar^2 g_J \frac{\Gamma_n \Gamma_\gamma}{\Gamma_n + \Gamma_\gamma}, \quad (2)$$

where $\lambdabar = \lambda / 2\pi$ is the reduced de Broglie wave length of the neutron, g_J is the resonance spin factor, and Γ_γ and Γ_n are the radiative and the neutron widths, respectively.

Because mass and geometry were precisely known for the ^{203}Tl sample, the ^{203}Tl(n, γ) yield could be determined accurately by applying the conventional saturated resonance method using the well-known 4.9 eV resonance in ^{197}Au [48,49], and the fact that the neutron flux of n_TOF EAR1 is known with an accuracy of 2% or better in the energy range between 1 eV and 10 keV [46]. Further details of the experimental setup and the analysis results for the

^{203}Tl(n, γ) measurement will be given in a separate publication [50].

Afterwards, f_N could be obtained for the ^{204}Tl-enriched sample by fixing the A_r of the newly measured four strongest ^{203}Tl resonances, which featured prominently in the yield due to the dominant content (96%) of ^{203}Tl.

Lastly, f_{th} in Eq. (1) accounts for the part of the capture spectrum missing under the pulse-height detection threshold, and it was calculated from MC simulations of the deexcitation cascades of ^{197}Au(n, γ), ^{203}Tl(n, γ), and ^{204}Tl(n, γ) [51]. Despite the relatively high threshold of 600 keV, necessary to reduce further the bremsstrahlung background arising from the ^{204}Tl β^--decay, the corresponding correction factors were less than 3% owing to the similarity in pulse-height spectra between the two Tl isotopes and gold.

For all samples, the resonance parameters were determined by analyzing $Y_{\exp}$ with the Bayesian R-matrix code SAMMY [52]. Once the normalization procedure was applied, a capture yield for ^{204}Tl(n, γ) could be obtained via Eq. (1). The ^{204}Tl enrichment and its associated uncertainty were evaluated by fitting the concentration of the daughter ^{204}Pb in the experimental yield, using the strongest resonance of ^{204}Pb and the corresponding parameters from Ref. [53].

A total systematic uncertainty of 12% was estimated for the experimental ^{204}Tl(n, γ) MACS calculated from resonances directly measured; partial contributions are summarized in Table II in the Supplemental Material [78].

The R-matrix analysis allowed us to identify eleven ^{204}Tl(n, γ) resonances, all below $E_n = 4$ keV. A problem is that higher E_n are involved in s-process nucleosynthesis in low mass AGB stars. Most of the neutrons are produced by the ^{13}C$(\alpha, n)^{16}$O reaction in the radiative ^{13}C pocket, in the upper part of the He intershell region, at temperatures corresponding to thermal energies of $kT \approx 8$ keV. A smaller amount of neutrons are also released by the partial activation of the ^{22}Ne$(\alpha, n)^{25}$Mg reaction at the bottom of the He intershell, where $kT \approx 25$–30 keV is reached during the recurrent convective thermal pulse (TP) events triggered by He fusion [6,54,55]. During TPs, the ^{22}Ne$(\alpha, n)^{25}$Mg may generate neutron densities in the order of $n_n \sim 10^{10}$–10^{11} cm^{-3} (orders of magnitude higher than in the ^{13}C pocket), and allows us to open several branching points along the s-process path [15,56,57].

To extend the MACS up to $kT \approx 30$ keV a methodology similar to that described in Ref. [35] was applied. From new average resonance parameters determined in the present experiment, and the simulation of random resonance sequences, the fraction of the total MACS at higher kT energies that could be measured in our experiment was determined.

Combining these calculated fractions with the directly measured contributions, the total MACS at each kT energy
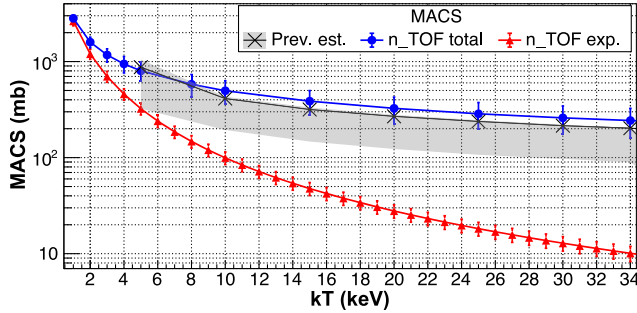
FIG. 2. MACS as a function of thermal energy (kT). Red solid triangles correspond to the contribution of observed resonances, whereas the blue solid circles represent the total MACS obtained in this work. The gray shadowed region indicates the range covered by previous theoretical estimations (see text for details), with the cross highlighting the calculation by Bao *et al.* [23].

was determined including its uncertainty. Further details on the procedure, the determination of average parameters, and the evaluation of the MACS uncertainty are provided in the Supplemental Material.

The total MACS as a function of kT is shown in Fig. 2. We obtained values of 580(168) mb and 260 (90) mb at $kT = 8$ keV and 30 keV, respectively (see the Supplemental Material for the values at other kT). Note that the observable contribution corresponds to about 25% in the first case, and 5% in the latter. The expected value of the total MACS at $kT = 30$ keV is about 20% higher than the KADONiS v0.3 recommended value of 215 mb from Bao *et al.*. The theoretical expected values of 175 mb from Rauscher and Thielemann [58] and 224 mb from TENDL-2021 [21] remain compatible within the quoted uncertainty. This is not the case for the values calculated by Harris (97 mb) [20] and Macklin (134 mb) [22]. In Figure 2 the shadowed region is used to represent the range of previous theoretical estimations, with the upper bound defined by TENDL-2021 and the lower bound by the value of Harris at 30 keV and its extrapolation to other kT by employing the energy dependence of TENDL-2021. The cross symbol corresponds to the values by Bao *et al.* [23].

To study the impact of the new ^{204}Tl MACS in the production of ^{204}Pb s-process nucleosynthesis, calculations were performed using NuGrid postprocessing codes applied to AGB stellar evolution simulations from MESA [59,60]. Our calculations, in which only the ^{204}Tl(n, γ) cross section was varied, included the simulations of the full AGB stage for stars with initial masses 1.65, 2, 3, and 4 $M_\odot$, all with metallicity $Z = 0.006$, which approximately corresponds to between one half and one third of the present value [10,61,62]. It is worth noting that although the present solar system s-process abundances are the outcome of the contribution of multiple generations of stars of different masses and metallicities [7,8,14,24], GCE calculations have confirmed that the dominant contribution to ^{204}Pb comes from the so-called main component of the s

process originating from low-mass AGB stars in the mass range of 1.5 to 3 $M_\odot$, with a minor contribution of only 2% expected from very low metallicity ($Z < 0.001$) AGB stars [7].

Hence, a more representative description of the main s-process abundances was obtained by calculating a weighted average (WA) of the 1.65, 2, and 3 $M_\odot$ NuGrid yields, applying the weights obtained from Salpeter's initial mass function (IMF) [63]. The weights assigned to each of the NuGrid models corresponded, respectively, to the fraction of stars between 1.5 and 1.8 $M_\odot$, between 1.8 and 2.5 $M_\odot$, and between 2.5 and 3.5 $M_\odot$, all normalized to the integral between 1.5 and 3.5 $M_\odot$.

The value of the WA was also compared to the simple average (SA) of the production yields of 1.65 and 3 $M_\odot$ AGB stars of half-solar metallicity, similar to the approach employed in the past to reproduce s-process abundances [12,15]. Note that no significant differences are expected in terms of s-process nucleosynthesis when using 1.65 $M_\odot$ instead of the 1.5 $M_\odot$ employed in [12]. To directly compare the calculated s-process yields with the solar s-only abundances, the ^{204}Pb yields are normalized to the production of the unbranched s-only isotope ^{150}Sm. This normalization is commonly used to directly compare s-process nucleosynthesis calculations with solar abundances [15,24,56]. Here, the use of the ratio $\rho_N = N(^{204}$Pb$)/N(^{150}$Sm$)$ allows one to have a preliminary estimate about the impact of the new MACS on the expected s-process production of ^{204}Pb before performing more detailed GCE calculations. Indeed, by means of this ratio the impact of some of the stellar physics and nuclear uncertainties equally affecting the production of both ^{150}Sm and ^{204}Pb can be minimized [15].

Fig. 3 shows the ratio ρ_N in the star envelope at the end of the AGB stage for the individual stars and for the two averaged combinations. Uncertainties were obtained by averaging correspondingly those of the separate stellar models. ρ_N was obtained for the MACS from this work and also for previous calculations by Harris [20], Rauscher and Thielemann [58], Bao *et al.* [23], and TENDL-2021 [21]. For simplicity, all calculated ratios have been normalized to the expected value of the ratio in the solar system of Lodders [10], which is derived from CI chondrites.

The MACS from this work yields a solar system normalized ratio $\rho_N = 0.97(+8, -6)$ for the WA, which is in agreement with Lodders without the need of additional contributions to ^{204}Pb.

We have also evaluated the impact of the uncertainty in the thermal dependency of the β^--decay rate of ^{204}Tl at stellar temperatures, for which we performed additional calculations with our MACS and the minimum and maximum β^--decay rates provided by [31]. By summing the MACS and the β^--decay uncertainties, we obtained a total uncertainty range for the normalized ρ_N of
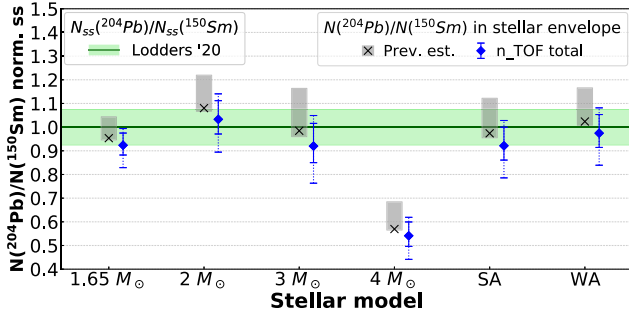
FIG. 3. Isotopic abundance ratios $N(^{204}\text{Pb})/N(^{150}\text{Sm})$ in the star envelope at the end of the AGB phase, obtained using the MACS from Fig. 2 for the stellar models described in the text. All values are normalized to the solar system (ss) ratio [10], which is highlighted by the thick green bar with the green shaded band depicting its uncertainty. Solid error bars reflect only the uncertainty contribution from the cross section, while dashed error bars include also the uncertainty on the thermal dependency of the β^- decay of ^{204}Tl [31].

$(+11, -14)$ for the WA. Note that future experiments like PANDORA [64] could provide valuable experimental constrains to this rate. The uncertainty in the thermal dependency for the much less frequent decay of ^{204}Tl to ^{204}Hg produced a negligible variation ($< 0.3\%$) in the final abundance of ^{204}Pb.

It is important to remark that the ^{204}Pb production (and therefore the $^{204}\text{Pb}/^{150}\text{Sm}$ ratio) becomes sensitive to the neutron density and the temperature conditions during the TP episodes which, in turn, influence the interplay between the MACS of ^{204}Tl and its temperature-dependent β^- decay at this s-process branching.

In this situation, some differences arising from the new ^{204}Tl MACS may be expected comparing different AGB stellar models. For instance, the choice of including convective-boundary mixing at the bottom of TPs [59] makes the He intershell in AGB models a bit hotter than other models without such a feature [65,66]. Among other things, this will affect the activation of s-process branchings, including ^{204}Tl [13]. The models shown in Fig. 3 can be used to gain some insight into these aspects. In comparison to the $3\,M_\odot$ star, the $1.65\,M_\odot$ model reaches lower TP temperatures. Thus, once the s-process path reaches ^{204}Tl lower neutron densities and capture rates are obtained with respect to the competing β-decay channel. This leads to a smaller spread in the $^{204}\text{Pb}/^{150}\text{Sm}$ ratio among different $^{204}\text{Tl}(n,\gamma)$ cross section values in the $1.65\,M_\odot$ model (see Fig. 3). Therefore, the final $^{204}\text{Pb}/^{150}\text{Sm}$ production ratio becomes sensitive to the different state-of-the-art AGB stellar sets. Hence, it would be of interest to perform similar calculations adopting the new ^{204}Tl MACS and its uncertainty with different AGB models [15,65–67].

Another important uncertainty directly affecting the neutron density is the cross section of $^{22}\text{Ne}(\alpha,\text{n})^{25}\text{Mg}$. Presently, several experimental efforts are indeed focused on the determination of both reactions' cross sections [68–71]. It is worth noting that some recent recommendations by Ota et al. [72] and Adsley et al. [68] based on recent data [73,74], apparently point to a $^{22}\text{Ne}(\alpha,\text{n})^{25}\text{Mg}$ cross section considerably lower than previous evaluations, including the one used in this work [75]. However, the new values are not generally accepted yet [76] and additional underground experiments [77] are expected to address these discrepancies.

To conclude, the neutron capture cross section of the s-process branching nucleus ^{204}Tl has been measured for the first time at energies relevant for nucleosynthesis in AGB stars. The high thermal neutron flux of ILL and the high resolution and luminosity of CERN n_TOF were key to producing a sufficient amount of ^{204}Tl and to resolving several $^{204}\text{Tl}(n,\gamma)$ resonances, respectively. New AGB nucleosynthesis calculations based on the MACS reported here are fully consistent with the observed solar abundance of ^{204}Pb and provide a more stringent constraint on its s-process contribution. Further insight on other possible contributions to the abundance of ^{204}Pb would require a corresponding improvement in the MACS of ^{204}Tl down to a level of about 10%, which would lead to a few percent uncertainty on the isotopic abundance of ^{204}Pb. Within the present experimental uncertainties, there is no need to invoke additional nucleosynthesis mechanisms or fractionation effects discussed previously in the literature in order to explain the ^{204}Pb abundance observed in the solar system.

[1] P. W. Merrill, Astrophys. J. **116**, 21 (1952).
[2] E. M. Burbidge, G. R. Burbidge, W. A. Fowler, and F. Hoyle, Rev. Mod. Phys. **29**, 547 (1957).
[3] A. G. W. Cameron, Stellar evolution, nuclear astrophysics, and nucleogenesis. Second edition, Technical Report, 1957.
[4] M. Busso, R. Gallino, and G. J. Wasserburg, Annu. Rev. Astron. Astrophys. **37**, 239 (1999).
[5] F. Käppeler, R. Gallino, S. Bisterzo, and W. Aoki, Rev. Mod. Phys. **83**, 157 (2011).
[6] A. I. Karakas and J. C. Lattanzio, Pub. Astron. Soc. Aust. **31**, e030 (2014).
[7] C. Travaglio, R. Gallino, M. Busso, and R. Gratton, Astrophys. J. **549**, 346 (2001).
[8] N. Prantzos, C. Abia, M. Limongi, A. Chieffi, and S. Cristallo, Mon. Not. R. Astron. Soc. **476**, 3432 (2018).
[9] C. Kobayashi, A. I. Karakas, and M. Lugaro, Astrophys. J. **900**, 179 (2020).
[10] K. Lodders, Space Sci. Rev. **217**, 44 (2021).
[11] J. J. Cowan, C. Sneden, J. E. Lawler, A. Aprahamian, M. Wiescher, K. Langanke, G. Martínez-Pinedo, and F.-K. Thielemann, Rev. Mod. Phys. **93**, 015002 (2021).
[12] C. Arlandini, F. Kappeler, K. Wisshak, R. Gallino, M. Lugaro, M. Busso, and O. Straniero, Astrophys. J. **525**, 886 (1999).
[13] M. Lugaro, F. Herwig, J. C. Lattanzio, R. Gallino, and O. Straniero, Astrophys. J. **586**, 1305 (2003).
[14] S. Bisterzo, C. Travaglio, R. Gallino, M. Wiescher, and F. Käppeler, Astrophys. J. **787**, 10 (2014).
[15] S. Bisterzo, R. Gallino, F. Käppeler, M. Wiescher, G. Imbriani, O. Straniero, S. Cristallo, J. Görres, and R. J. deBoer, Mon. Not. R. Astron. Soc. **449**, 506 (2015).
[16] J. N. Connelly, M. Bizzarro, A. N. Krot, Åke Nordlund, D. Wielandt, and M. A. Ivanova, Science **338**, 651 (2012).
[17] J. Connelly, J. Bollard, and M. Bizzarro, Geochim. Cosmochim. Acta **201**, 345 (2017).
[18] T. Watanabe, G. E. Stokes, and R. P. Schuman, *Neutron Cross Sections and Technology*, edited by D. T. Goldman (National Bureau of Standards, Washington, D.C., 1968), pp. 893–6.
[19] I. Dillmann, M. Heil, F. Käppeler, R. Plag, T. Rauscher, and F. Thielemann, AIP Conf. Proc. **819**, 123 (2006).
[20] M. J. Harris, Astrophys. Space Sci. **77**, 357 (1981).
[21] A. Koning, D. Rochman, J.-C. Sublet, N. Dzysiuk, M. Fleming, and S. van der Marck, Nucl. Data Sheets **155**, 1 (2019).
[22] R. L. Macklin and R. R. Winters, Astrophys. J. **208**, 812 (1976).
[23] Z. Bao, H. Beer, F. Käppeler, F. Voss, K. Wisshak, and T. Rauscher, At. Data Nucl. Data Tables **76**, 70 (2000).
[24] S. Cristallo, C. Abia, O. Straniero, and L. Piersanti, Astrophys. J. **801**, 53 (2015).
[25] T. Rauscher, A. Heger, R. D. Hoffman, and S. E. Woosley, Astrophys. J. **576**, 323 (2002).
[26] T. Rauscher, N. Dauphas, I. Dillmann, C. Fröhlich, Z. Fülöp, and G. Gyürky, Rep. Prog. Phys. **76**, 066201 (2013).
[27] M. Pignatari, K. Göbel, R. Reifarth, and C. Travaglio, Int. J. Mod. Phys. E **25**, 1630003 (2016).
[28] C. Travaglio, T. Rauscher, A. Heger, M. Pignatari, and C. West, Astrophys. J. **854**, 18 (2018).
[29] G. Gonzalez, Mon. Not. R. Astron. Soc.: Lett. **443**, L99 (2014).
[30] K. Takahashi and K. Yokoi, At. Data Nucl. Data Tables **36**, 375 (1987).
[31] S. Goriely, Astron. Astrophys. **342**, 881 (1999), https://ui.adsabs.harvard.edu/abs/1999A&A...342..881G.
[32] C. Lederer et al. (n_TOF Collaboration), Phys. Rev. Lett. **110**, 022501 (2013).
[33] J. Lerendegui-Marco et al., EPJ Web Conf. **279**, 13001 (2023).
[34] S. Marrone et al. (n_TOF Collaboration), Phys. Rev. C **73**, 034604 (2006).
[35] C. Guerrero et al. (n_TOF Collaboration), Phys. Rev. Lett. **125**, 142701 (2020).
[36] C. Guerrero et al. (The n_TOF Collaboraiton), Eur. Phys. J. A **49**, 27 (2013).
[37] N. Colonna, F. Gunsing, and F. Käppeler, Prog. Part. Nucl. Phys. **101**, 177 (2018).
[38] J. Lerendegui-Marco et al. (n_TOF Collaboration), Phys. Rev. C **97**, 024605 (2018).
[39] R. Plag, M. Heil, F. Käppeler, P. Pavlopoulos, R. Reifarth, and K. Wisshak, Nucl. Instrum. Methods Phys. Res., Sect. A **496**, 425 (2003).
[40] R. L. Macklin and J. H. Gibbons, Phys. Rev. **159**, 1007 (1967).
[41] J. L. Taín et al., J. Nucl. Sci. Technol. **39**, 689 (2002).
[42] U. Abbondanno et al. (n_TOF Collaboration), Nucl. Instrum. Methods Phys. Res., Sect. A **521**, 454 (2004).
[43] S. Agostinelli et al., Nucl. Instrum. Methods Phys. Res., Sect. A **506**, 250 (2003).
[44] J. Allison et al., IEEE Trans. Nucl. Sci. **53**, 270 (2006).
[45] J. Allison et al., Nucl. Instrum. Methods Phys. Res., Sect. A **835**, 186 (2016).
[46] M. Barbagallo et al. (The n_TOF Collaboraiton), Eur. Phys. J. A **49**, 156 (2013).

[47] S. F. Mughabghab, *Atlas of Neutron Resonances (Sixth Edition)* (Elsevier, New York, 2018).

[48] R. L. Macklin, J. Halperin, and R. R. Winters, Nucl. Instrum. Methods **164**, 213 (1979).

[49] C. Massimi *et al.* (n_TOF Collaboration), Phys. Rev. C **81**, 044616 (2010).

[50] A. Casanovas *et al.* (to be published).

[51] A. Casanovas-Hoste, Neutron capture cross section measurement of the heaviest s-process branching ^{204}Tl and of ^{203}Tl at CERN n_TOF, Ph.D. thesis, 2020.

[52] N. M. Larson, Updated user's guide for SAMMY: Multilevel R-matrix fits to neutron data using Bayes' equations, Technical Report, Oak Ridge National Laboratory, 2008.

[53] C. Domingo-Pardo *et al.* (n_TOF Collaboration), Phys. Rev. C **75**, 015806 (2007).

[54] O. Straniero, R. Gallino, M. Busso, A. Chiefei, C. M. Raiteri, M. Limongi, and M. Salaris, Astrophys. J. Lett. **440**, L85 (1995).

[55] F. Herwig, Annu. Rev. Astron. Astrophys. **43**, 435 (2005).

[56] R. Gallino, C. Arlandini, M. Busso, M. Lugaro, C. Travaglio, O. Straniero, A. Chieffi, and M. Limongi, Astrophys. J. **497**, 388 (1998).

[57] M. Lugaro, A. M. Davis, R. Gallino, M. J. Pellin, O. Straniero, and F. Käppeler, Astrophys. J. **593**, 486 (2003).

[58] T. Rauscher and F.-K. Thielemann, At. Data Nucl. Data Tables **75**, 1 (2000).

[59] C. Ritter, F. Herwig, S. Jones, M. Pignatari, C. Fryer, and R. Hirschi, Mon. Not. R. Astron. Soc. **480**, 538 (2018).

[60] B. Paxton, L. Bildsten, A. Dotter, F. Herwig, P. Lesaffre, and F. Timmes, Astrophys. J. Suppl. Ser. **192**, 3 (2010).

[61] E. Magg *et al.*, Astron. Astrophys. **661**, A140 (2022).

[62] M. Asplund, N. Grevesse, A. J. Sauval, and P. Scott, Annu. Rev. Astron. Astrophys. **47**, 481 (2009).

[63] E. E. Salpeter, Astrophys. J. **121**, 161 (1955).

[64] D. Mascali *et al.*, Universe **8**, 80 (2022).

[65] S. Cristallo, L. Piersanti, O. Straniero, R. Gallino, I. Domínguez, C. Abia, G. D. Rico, M. Quintini, and S. Bisterzo, Astrophys. J. Suppl. Ser. **197**, 17 (2011).

[66] A. I. Karakas and M. Lugaro, Astrophys. J. **825**, 26 (2016).

[67] M. Busso, D. Vescovi, S. Palmerini, S. Cristallo, and V. Antonuccio-Delogu, Astrophys. J. **908**, 55 (2021).

[68] P. Adsley *et al.*, Phys. Rev. C **103**, 015805 (2021).

[69] R. Talwar, T. Adachi, G. P. A. Berg, L. Bin, S. Bisterzo *et al.*, Phys. Rev. C **93**, 055803 (2016).

[70] R. Longland, C. Iliadis, and A. I. Karakas, Phys. Rev. C **85**, 065809 (2012).

[71] Shahina *et al.*, Phys. Rev. C **106**, 025805 (2022).

[72] S. Ota, G. Christian, W. N. Catford, G. Lotay, M. Pignatari *et al.*, Phys. Rev. C **104**, 055806 (2021).

[73] H. Jayatissa *et al.*, Phys. Lett. B **802**, 135267 (2020).

[74] S. Ota *et al.*, Phys. Lett. B **802**, 135256 (2020).

[75] M. Jaeger, R. Kunz, A. Mayer, J. W. Hammer, G. Staudt, K. L. Kratz, and B. Pfeiffer, Phys. Rev. Lett. **87**, 202501 (2001).

[76] M. Wiescher, R. J. deBoer, and J. Görres, Eur. Phys. J. A **59**, 11 (2023).

[77] D. Rapagnani, C. Ananna, A. Di Leva, G. Imbriani, M. Junker, M. Pignatari, and A. Best, EPJ Web Conf. **260**, 11031 (2022).

[78] See Supplemental Material at http://link.aps.org/supplemental/10.1103/PhysRevLett.133.052702 for a list of the ^{204}Tl(n, γ) MACS values obtained in this work. In addition, a more detailed description of the semi-empirical procedure employed to derive the MACS is given. We also provide a summary of the different contributions to the total systematic uncertainty reported in the main manuscript. Finally, the *R*-Matrix fit with SAMMY of a new ^{204}Tl(n, γ) resonance is shown as an example of the resonance fit results.